http://dx.doi.org/10.5012/bkcs.2012.33.6.1900

Synthesis, Characterization, Absorbance, Fluorescence and Non Linear Optical Properties of Some Donor Acceptor Chromophores

Abdullah M. Asiri,[†,‡] Salman A. Khan,[†,*] Muhammed S. Al-Amoudi,[§] and Kalid A. Alamry[†]

[†]*Chemistry Department, Faculty of Science, King Abdulaziz University, P.O. Box 80203, Jeddah, Saudi Arabia 21589*
[*]*E-mail: sahmad_phd@yahoo.co.in*
[‡]*Center of Excellence for Advanced Materials Research, King Abdulaziz University, P.O. Box 80203, Jeddah, Saudi Arabia 21589*
[§]*Chemistry Department, Faculty of Science, Taif University, P.O. Box 888, Taif 21589, Saudi Arabia*
Received February 6, 2012, Accepted March 12, 2012

Three carbazole chromophores featuring dicyano, cyano, ethyl acetate and dimethyl acetate groups as an acceptor moiety with a π-conjugated spacer and *N*-methyl dibenzo[*b*]pyrole as donor were synthesized by Knovenagel condensation and characterized by IR, ^{1}HNMR, ^{13}CNMR, UV-vis, fluorescence spectroscopy, electrochemistry and theoretical B3LYP/6-311G* level whilst NLO properties and spectroscopic quantities were calculated. Calculations showed remarkable trend with HOMO located on the donor moiety and LUMO on the acceptors dicyano methylene, cyano, ethyl acetate methylene and dimethyl acetate methylene. In agreement with the calculations, solvatochromic, behavior intramolecular charge transfer band was observed in the visible region.

Key Words : Knovenagel condensation, Carbazole aldehyde, Pyridine, NLO Chromophore

Introduction

Carbazole derivatives have been well known dyes which are characterized by efficient fluorescence emission and well define electronic absorption and fluorescence transition dipole moments.[1,2] As a consequence, they have attracted considerable attention of researchers working in the area of pure and applied sciences. Because of their high photostability and the elongated molecular shape, carbazole derivatives can be applied as probes in the experimental studies of molecular orientational order in thermotropic and lyotropic liquid crystals, in liquid-crystalline polymers, and in lipid membranes.[3,4] Most of the carbazole derivatives have been considered for applications in organic electronic devices and in optical disks.[5-7] They can be also applied as a fluorescent component in liquid crystal displays working in passive or active modes.[8] Carbazole dyes present a wide range of colors so they are applied in high grade paints utilized in automotive industry finishes for example.[9] At certain conditions, the molecules of carbazole derivatives can aggregate forming crystalline or semicrystalline two-dimensional structures. The aggregation properties of these molecules are strongly dependent on the chemical structure of the substituents in carbazole skeleton, solvent, the concentration of the dye, and some physical parameters, such as temperature.[10] Langmuir and Langmuir-Blodgett (LB) films are examples of such two-dimensional systems in which aggregation is observed.[11] Due to wild application of carbazole skeleton we have synthesized a novel series of donor acceptor carbazole derivatives from the carbazole aldehyde with activated methylene group by the Knovenagel condensation and their absorption and fluorescence studies in different solvents.

Experimental

Carbazole aldehyde and activated methylene have used from Acros Organic and used without further purification. Other solvents (A.R.) and reagents were obtained commercially and used without further purification except chloroform, ethanol and methanol. Melting points were recorded on a Thomas Hoover capillary melting apparatus without correction. IR spectra were taken on KBr disks on a Nicolet Magna 520 FTIR spectrometer, ^{1}H-NMR and ^{13}C-NMR were recorded in $CDCl_3$ on a Brucker DPX 600 MHz spectrometer using TMS as internal standard. The UV-vis absorption measurements were acquired by use of a Perkin-Elmer UV-vis scanning spectrophotometer. Absorption spectra were collected using a 10 mm quartz cuvet. Fluorescence measurements were performed using a Perkin-Elmer luminescence spectrofluorometer equipped with a 20-KW for 8 μs duration xenon lamp and gated photomultiplier tube (PMT) and red-sensitive R928 PMT detectors.

Cyclic voltammetry measurements were made using a conventional three electrode cell configuration linked to an *EG & G* model 283 Potentiostat. The platinum electrode surface was 7.85×10^{-3} cm^2 as a working electrode, coiled platinum wire as a counter electrode and saturated Ag/AgCl as a reference electrode.

The potential was calculated with relative to the Ag/AgCl reference electrode at 25 °C. and 0.1 mol/L tetraethyl ammonium chloride (*TEACl*) as background electrolyte. Cyclic voltammograms were recorded after background subtraction and iR compensation to minimize double-layer charging current and solution resistance. The working electrode was polished on a polisher Ecomet grinder. Cyclic voltammetric data were obtained at scan rate ranging from 0.02 to 5 V/s in

non aqueous media at (25 ± 2) °C. All working solutions were thoroughly degassed with oxygen free nitrogen and a nitrogen atmosphere was maintained above the solution throughout the experiments.

General Procedure for the Synthesis of Carbazole Derivatives. A mixture of carbazole aldehyde (0.0058 mol) and corresponding active methylene (0.0058 mol) in anhydrous ethanol (15 mL), in the presence of few drops of pyridine was refluxed at 80 °C for 3h with continuous stirring. Progress of reaction was monitored by TLC. After completion of the reaction the solution was cooled. The heavy precipitate thus obtained was collected by filtration and purified by recrystallization from a mixture of methanol and chloroform.

2-(9-Ethyl-9*H*-carbazol-3-ylmethylene)-malononitrile (1): IR (KBr) ν_{max} cm^{-1}: 1561 (C=C), 1168 (C-N), 2218 (CN), 2980 (C-H, aliphatic), 3058 (C-H, aromatic). ^{1}H-NMR ($CDCl_3$) δ 8.08 (H1, d, *J* = 1.2 Hz), 8.14 (H2, d, *J* = 7.8 Hz), 8.62 (H3, s), 7.49 (H4, d, 7.49, *J* = 7.8 Hz), 7.56 (H5, dd, *J* = 7.8 Hz), 7.32 (H6, dd, *J* = 7.8 Hz), 7.46 (H7, d, *J* = 7.2 Hz), 7.56 (H8, s), 4.43 (t, CH_3-CH_2-N, *J* = 14.4 Hz), 1.49 (CH_3-CH_2-N, q, *J* = 7.2 Hz); ^{13}C-NMR ($CDCl_3$) δ 191.88, 160.19, 143.38, 140.71, 128.38, 127.40, 125.19, 123.75, 122.34, 121.34, 115.15, 114.19, 109.41, 77.23, 76.35, 38.11, 13.89, 1.02.

2-Cyano-3-(9-ethyl-9*H*-carbazol-3-yl)-acrylic Acid Ethyl Ester (2): IR (KBr) ν_{max} cm^{-1}: 1720 (C=O), 1562 (C=C), 1158 (C-N), 2216 (CN) 2929 (C-H, aliphatic), 2975 (C-H, aromatic), ^{1}H-NMR ($CDCl_3$) δ 8.16 (H1, d, *J* = 7.8 Hz), 8.22 (H2, d, *J* = 7.2 Hz), 8.40 (H3, s), 7.44 (H4, d, *J* = 4.2 Hz), 7.32 (H5, dd, *J* = 7.2 Hz), 7.55 (H6, dd, *J* = 7.8 Hz), 7.44 (H7, d, *J* = 4.2 Hz), 8.73 (H8, s), 4.41 (CH_3-C<u>H</u>$_2$-N, t, *J* = 14.4 Hz), 1.46 (C<u>H</u>$_3$-CH_2-N, q, *J* = 7.2 Hz), 4.41 (CH_3-C<u>H</u>$_2$-O), 1.46 (C<u>H</u>$_3$-CH_2-O, t); ^{13}C-NMR ($CDCl_3$) δ 163.68, 162.44, 157.67, 156.00, 142.33, 140.57, 130.88, 129.24, 125.46, 123.54, 120.78, 109.41, 100.89, 97.55, 77.51, 62.42, 58.49, 37.96, 18.44, 14.29.

2-(9-Ethyl-9*H*-carbazol-3-ylmethylene)- Malonic Acid Diethyl Ester (3): IR (KBr) ν_{max} cm^{-1}: 1678 (C=O), 1589 (C=C), 1147 (C-N), 1231 (C-O), 2973 (C-H, aliphatic), 3053 (C-H, aromatic) ^{1}H-NMR ($CDCl_3$) δ 8.00 (H1, d, *J* = 1.2 Hz), 8.16 (H2, d, *J* = 7.8 Hz), 7.20 (H3, s), 7.47 (H4, d, *J* = 6.0 Hz), 7.55 (H5, dd, *J* = 7.2 Hz), 7.31 (H6, dd, 7.2 Hz), 7.47 (H7, d, *J* = 7.8 Hz), 8.61 (H8, s), 4.42 (CH_3-CH_2-N, t, *J* = 14.4 Hz), 1.48 (CH_3-CH_2-N, q, *J* = 7.2 Hz), 1.30 (CH_3-COO, s). ^{13}C-NMR ($CDCl_3$) δ 8.06, 146.20, 144.39, 143.54, 140.64, 127.19, 126.44, 124.07, 123.10, 121.20, 114.29, 108.68, 77.23, 52.55, 51.59, 37.92, 37.76, 18.44, 13.94, 13.83.

Result and Discussion

The synthesis of carbazol derivatives are straight forward and the compounds were isolated in good yield. The derivatives were synthesized by using the literature procedure.[12] The obtained compounds are stable in the solid state as well as in the solution. The physical data of the compounds **1-3** are given in Table 1. The structure of all the compounds presented in experimental section was established by comparing spectral data (IR, ^{1}H-NMR & ^{13}C-NMR). Assignments of selects characteristic IR band positions provide significant indication for the formation of the carbazole derivatives. The compounds showed intense bands at 1554-1590 cm^{-1} due to *v* (C=C) stretch, which is confirm the formation of donor accepter dyes derivatives.

Table 1. Physical data of compounds (**1-3**)

Compound no.	Solvent	Yield (%)	mp (°C)	Molecular formula
1	$CHCl_3$	35.12	169	$C_{18}H_{13}N_3$
2	$CHCl_3$	28.25	112	$C_{20}H_{18}O_2N_2$
3	$CHCl_3$	35.00	150	$C_{20}H_{19}NO_4$

Further evidence for the formation of carbazole derivatives was obtained from the ^{1}H-NMR spectra, which provide diagnostic tools for the positional elucidation of the protons. Assignments of the signals are based on the chemical shifts and intensity patterns. The aromatic protons of carbazole derivatives are shown as *s*,*d* and *dd* in the range (7.02-8.62) ppm for the compounds. A Singlet due to =C-H proton in the compounds was observed at (7.56-8.73) ppm respectively.

Absorption and Emission Spectra. Electronic absorption spectra of carbazole derivatives were measured in chloroform and acetonitrile (Figs. 1-6). The absorption maximum for the three compounds appears at 335-417 nm while its fluorescence emerges at 418-519 nm in chloroform as shown.

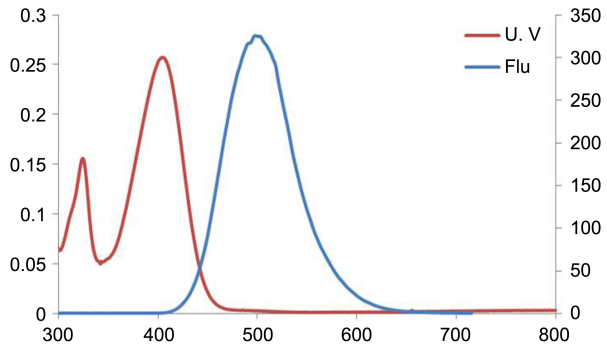

Figure 1. Absorption and emission spectra of compound **1** in acetonitrile at room temperature.

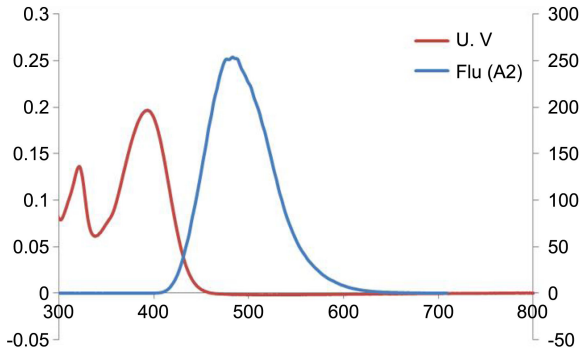

Figure 2. Absorption and emission spectra of compound **2** in acetonitrile at room temperature.

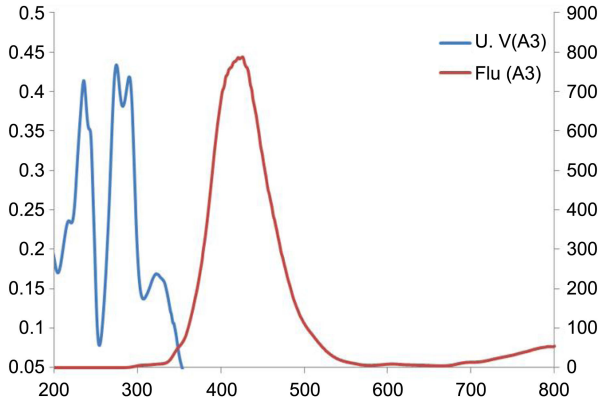

Figure 3. Absorption and emission spectra of compound **3** in acetonitrile at room temperature.

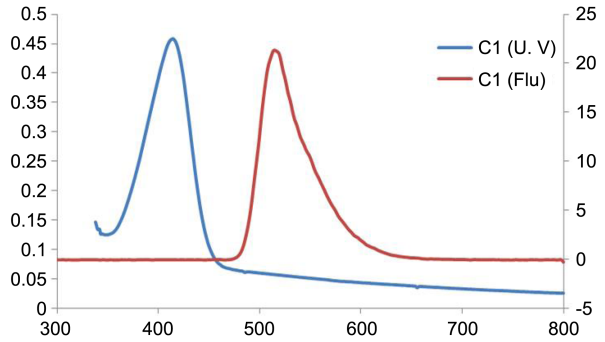

Figure 4. Absorption and emission spectra of compound **1** in chloroform at room temperature.

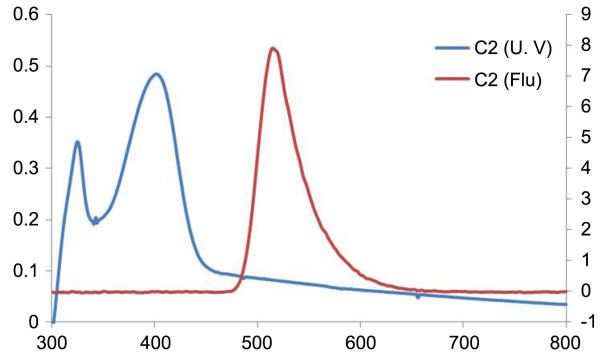

Figure 5. Absorption and emission spectra of compound **2** in chloroform at room temperature.

The maxima of the absorption and emission wavelength in acetonitrile and chloroform. As a typical of charge-transfer transition, an increase in the polarity of the medium leads to red shift of the absorption maximum. The absorption and emission bands become broader and structure less, in **2** and **3**, due to specific solute-solvent interaction.

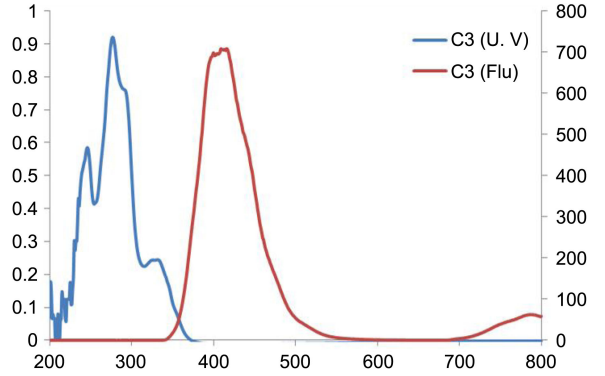

Figure 6. Absorption and emission spectra of compound **3** in chloroform at room temperature.

Electrochemical Analysis of the NLO Chromophores. We run electrochemical analysis to measure the redox ionization potential, the peak characteristics to identify the nature of the electrode reaction and to determine the number of electrons consumed in electro-oxidation & electro-reduction of the chromophores. The new compounds were characterized by cyclic voltammetry in $CHCl_3$ solution for estimating the energy levels of the organic NLO chromophores Tables 2-4 and (Figs. 4-6). The oxidation process corresponds to the removal of electrons from the highest occupied molecular orbitals (HOMO), whereas the reduction cycle corresponds to fill the lowest unoccupied molecular orbital (LUMO) by electrons. Therefore, the oxidation and reduction potentials are related to the energies of HOMO and LUMO levels of an organic NLO molecule and can provide useful information regarding the magnitude of the energy gap. Figure 8 shows the cyclic voltammograms of compounds **1**, **2** and **3**. They exhibit a single reversible oxidative wave in a positive energy and an irreversible reductive peak in a negative energy indicating the EC mechanism is follow in the case of reduction process. Usually, HOMO-LUMO gaps can be estimated from the oxidation

Table 2. Electrochemical and spectroscopic data of the compounds (**1-3**)

Compounds	$E_{ox}^{1/2}$	E_{HUMO} (eV)	E_{LUMO} (eV)	$\Delta E_{spect.}$ (eV)	$\lambda_{cut\text{-}off}$ (nm)
1	0.772	–5.172	–2.880	2.291	542
2	0.781	–5.181	–2.469	2.712	458
3	0.762	–5.162	–1.859	3.303	376

Table 3. Peak characteristics of the investigated carbazole derivatives at scan rate 1 V/s

Compound	Ep, V		Ep-Ep/2		ΔEp		Peak area × 10^5 (A.V)	
	Red	Oxid	Red	Oxid	Red	Oxid	Red	Oxid
1	–0.702	0.358	0.394	0.247	–	0.420	4.8	9.6
2	–0.682	0.372	0.383	0.226	–	0.391	4.6	9.7
3	–0.656	0.372	0.365	0.235	–	0.383	5.01	11.0

Table 4. Electronic absorption and emission spectral data and calculated microscopic nonlinear optical parameters of the compounds (**1-3**)

	Abs. λ_{max} (nm), ε ($M^{-1}cm^{-1}$)		Em. λ_{max} (nm)		Theoretical data		
	$CHCl_3$	Ac	$CHCl_3$	Ac	μ (× 10^{-18} esu)	β(0) (× 10^{-30} esu)	μβ(0) (× 10^{-48} esu)
1	417 (33630)	407 (23370)	517	504	6.79	269	1826
2	403 (32450)	396 (21680)	519	488	7.35	175	1286
3	335 (19640)	329 (15310)	426	418	5.44	82	446

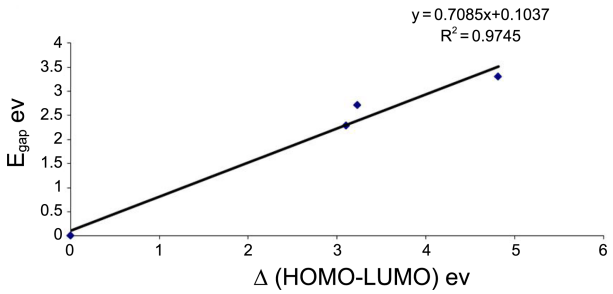

Figure 7. Linear correlation between E_{gap} (determined from λ_{max} and (HOMO-LUMO).

and reduction potentials. However, the reduction peaks are not clear to determine accurately the ionization potential and thus we have to employ the optical energy gap from the absorption edge of the electronic spectrum.[13] Although there is delocalization between the carbazoles moiety and the substituents, the redox properties can considered in terms of the energy levels for reduction process as:

$$Car + e \longleftrightarrow Car^{--}$$

and for oxidation process as:

$$Car - e \overset{E^{o'}_1}{\longleftrightarrow} Car^{\cdot +}$$

$$Car - e \overset{E^{o'}_2}{\longleftrightarrow} Car^{++}$$

In the case of molecules in which the electrons are added to or removed from a molecular orbital delocalized over the entire molecule, the energy required for the addition (or removal) of the second electron must be greater than that required for the addition (or removal) of the first electron step. Analysis of the cyclic voltammograms in terms of the two one electron process showed that the change in the carbazole geometry in reduction process. The three carbazole derivatives exhibited single two-electron process. This was attributed to a slight negative shift of the redox potential of the second electron transfer due to the preferential salvation of carbazole species by acetonitrile.[14]

The reduction potentials of dicyno **1** and cyno, ethyl acetate **2** shift negatively compared to that of **3** (dimethyl acetate groups). This indicates that the reduction in **3** originates from the acceptor moiety dimethyl acetate with π-conjugated spacer.[15,16] Thus, as shown in Table 2, the relatively smaller HOMO-LUMO gap of **3** compared to that of **1** and **2** is ascribed to the much lower than the lowest unoccupied molecular orbital (LUMO) energy level of **3**.

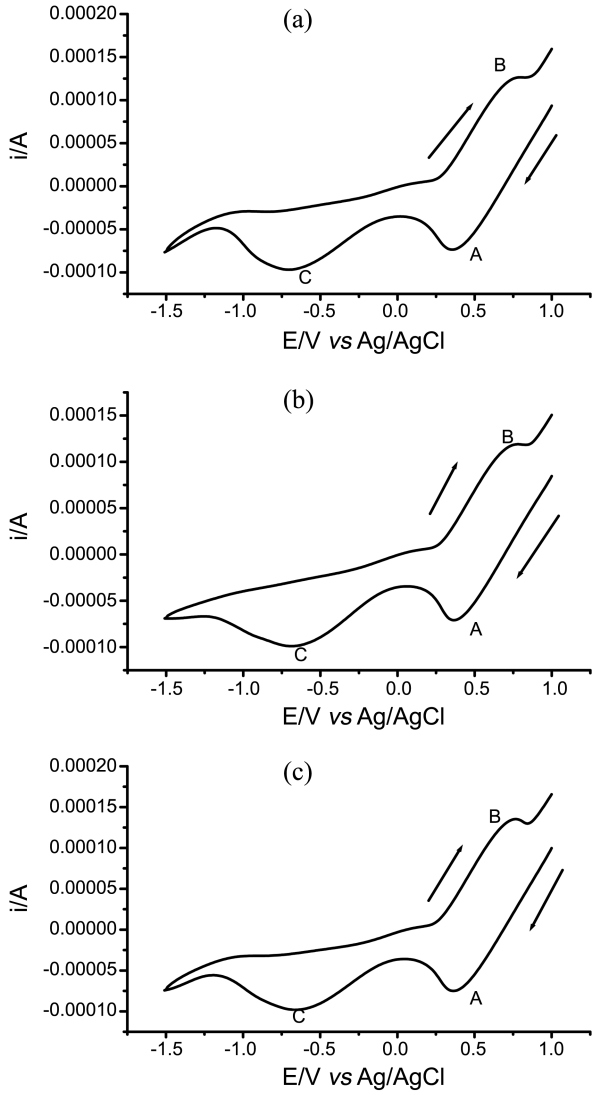

Figure 8. Cyclic voltamograms of compound **1** (a), compound **2** (b) and compound **3** (c) in acetonitryl.

The results shown in Figure 9 present the plot of charge (Q) versus the potential which indicate that the asymmetry of the charges in the forward and backward scan confirming the presence of chemical process after electron transfer of reduction step. In the case of oxidation process the charge in the forward scan is equal to the charge in the backward scan confirming the absence of chemical process coupled with electron transfer *i.e* simple electron transfer.[17] The plot of convoluted current at the end of the return scan $I_{1(end)}$ *vs* $v^{1/2}$

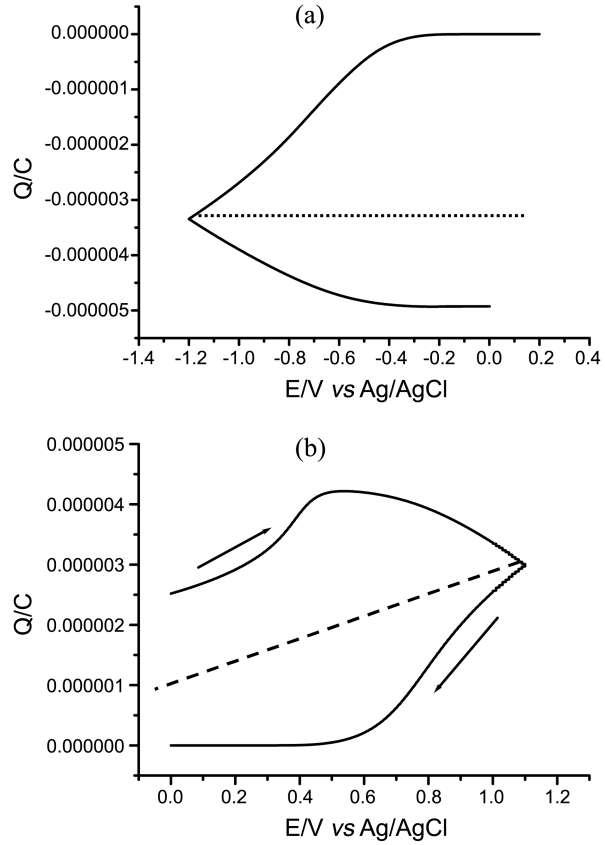

Figure 9. Plot of Q *versus* the applied potential of carbazole derivative **1** for reduction process (a) and for oxidation process (b).

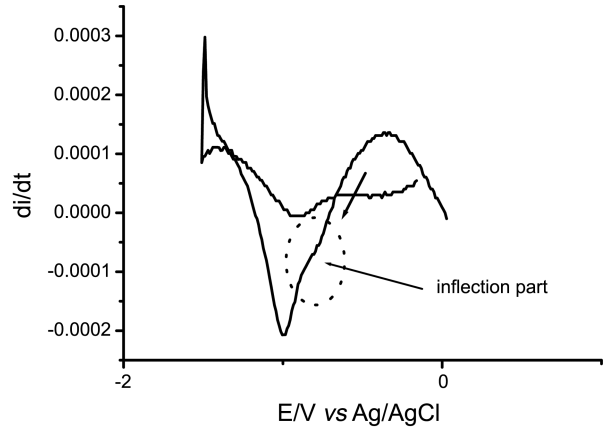

Figure 10. Plot of current (di/dt) *versus* potential of the carbazole derivative **1** of reduction process.

of the reduction process is shown in Figure 10. As shown the plot exhibited that the values of $I_{1(end)}$ decrease with increasing the sweep rate which indicates the EC nature of reduction process.[18] This plot is simple and new route for identification of the nature of electrode reaction.

The differentiation of current (di/dt) *vs* the applied potential of the reduction process of compound **1** is shown in Figure 11. The plot displayed a small inflection of the reduction peak in the forward direction at potential −0.81 V at scan rate of 1 V/s. This behavior indicates and confirms

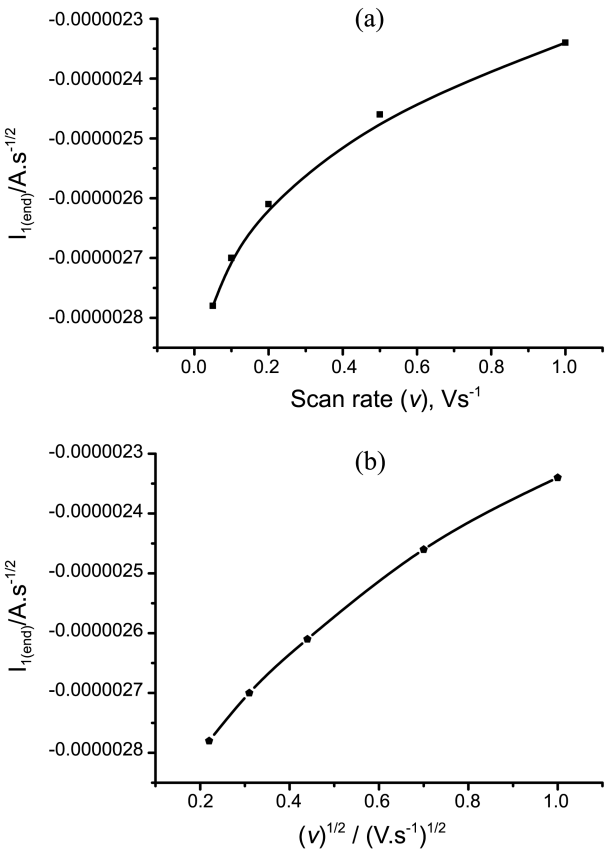

Figure 11. Plot of convoluted current at the end of scan ($I_{1(end)}$) versus scan rate (v) (a) and ($I_{1(end)}$) versus square root of scan rate ($v^{1/2}$) (b) of the reductive peak of compound **1**.

that the reduction process involves two one electron. Also the integration of peaks for oxidation and reduction processes revealed that peak area in case of reduction process is half that of the peak area in case of oxidation process. The calculation of peak areas indicate that the overall number of electrons involved in reduction process is equal to that involved in oxidation process. Table 3 summarize the peak characteristics of the carbazole derivatives **1-3** and indicates the sluggish nature of electrode reaction. The number of electrons consumed in electrode reaction were calculated

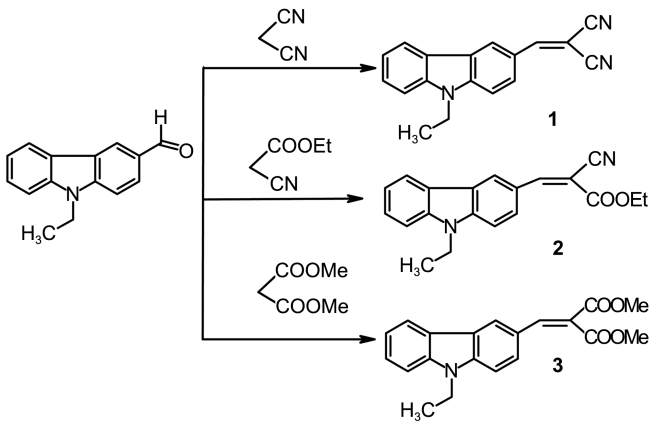

Scheme 1. Schematic diagram showing the synthesis of compounds (**1-3**).

Table 5. Calculated oscillator strength (f), radiative rate constant, transition dipole length <r> and energy of the first excited E (S_1) in $CHCl_3$ for the compounds (**1-3**)

Compound no.	f (unitless)	k_{er} (sec^{-1})	<r> (10^{-8} cm)	E_{S_1} (kJ mol^{-1})
1	0.48	2.7×10^8	1.4	257
2	0.58	3.6×10^8	1.5	246
3	0.38	3.4×10^8	1.1	326

and confirmed *via* the following equation.[19]

$$n = \frac{(dI_1/dt)_{max}}{(I_{lim}\alpha)\ 11.567}$$

Where $(dI_1/dt)_{max}$ is peak height of the deconvoluted current and the other terms have their usual meaning. The number of electrons was found to be 1.92 *i.e* = 2.0 for both oxidation and reduction process.

The electrochemical analysis is collected in Table 2 including the data from spectroscopic measurements.

The absorption spectroscopic data and the cyclic voltammetry are entirely consistent with an increase in electron delocalization when the acceptor is a cyano group. When we compare the LUMO levels of compound **1** and **3**, acceptor strength of the cyano groups was proven to be larger than that of the carboxyl and can be used for NLO application. HOMO levels did not show large difference because we used the same donor.

Oscillator Strength and Transition Dipole Moment. The oscillator strength *f* of clearly defined transition can be calculated from the UV/vis spectra Table 5. For fully-allowed transition, *f* equals 1 and for forbidden transitions *f* ~ 0.1. The value of *f* can be calculated from the following equation.[20]

$$f = \varepsilon_{max}\,\Delta\bar{\nu}_{1/2}/2.5 \times 10^8\,(\text{unitless})$$

$$f = 4.32 \times 10^{-9} \int \varepsilon(v) d\,v \qquad (1)$$

or $$f = 4.32 \times 10^{-9}\,\Delta\nu_{1/2}\,\varepsilon_{max}$$

Where $\Delta\nu_{1/2}$ is the width of absorption band in cm^{-1} at half ε_{max}

The length (in cm) of the dipole moment **r** (*i.e*., er is the transition dipole moment) can be expressed by

$$r^2 = \varepsilon_{max}\,\Delta\nu_{1/2}/2.5 \times 10^{19}\,\nu \qquad (2)$$

The radiation decay rate constant (k_r) a fluorophore was calculated from the modified Strickler-Berg relation.

$$k_r = 1/\tau_o = 2.88 \times 10^{-9}\,n^2 <\nu> \qquad (3)$$

Where *n* is the refraction index of the solvents ν^2_m is the energy of absorption maximum (cm^{-1}) and the integration is the area under absorption peak.

Nonlinear Optical Properties. The first hyperpolarizability of the chromophores can be calculated from the solvatochromic method according to Eq. (3).[21-24]

Table 6. Calculated orbital energies in eV, based on the B3LYP/6-311G* level

	HOMO	LUMO	H-L	D. M.
1	−0.22656	0.09835	−0.32491	10.3155
2	−0.21793	−0.08506	−0.13287	8.6479
3	−0.21044	−0.06536	−0.14508	5.3235

$$\beta CT\mu g = 4.612 \times 10^{-5} \times f(\lambda)\varepsilon\,\Delta\bar{\nu}_{1/2}\,\Delta a^3/\Delta f$$

$$f(\lambda) = \lambda^3\,\lambda_0{}^4/(\lambda_0{}^2 - 4\lambda^2)\,(\lambda_0{}^2 - \lambda^2) \qquad (4)$$

$$f(D) = 2\,(D-1)\,2D + 1$$

where λ is the maximum absorption wavelength of the molecule in excited state, and here it is assumed to b the maximum absorption wavelength of molecule in dipolar solvent; ε, $\Delta\bar{\nu}_{1/2}$, $\Delta\bar{\nu}$ and λ_0 are maximum of absorption coefficient in dipolar solvent, the difference of peaks at the middle, shift of maximum absorption in different solvents and wave length of base frequency (1064 nm), respectively.

Optical *vs*. Electrochemical HOMO-LUMO Gap. A plot of optical band gap, calculated from λ_{max} in the UV/vis spectrum, against the difference between the HOMO and LUMO in CV shows a linear correlation (R = 0.974) between the two quantities Figure 10. This indicates that the same orbitals are involved in electrochemistry and in absorption spectroscopy. A decrease in the band gap of 0.591 eV for the introduction of a cyano group and 0.739 eV for the introduction of a second cyano group (compare compound 3). The decrease of the HOMO-LUMO gap can therefore be mainly attributed to the larger lowering of the LUMO level rather than to the elevation of the HOMO level.

Theoretical Calculations. The replacement of the carboxyl group by cyano causes a more positive potential for the oxidation of the molecule. From compound **2** (one CN) to **1** (two CNs), the observed shifts of the oxidation potential are +40 mV and +60 mV respectively compared to compound **1** (Table 6).

Calculations on B3LYP/6-311G* level predicted that λ_{max} for compound **1** would be the most red shifted, followed by compound **3** and **2** respectively. This order was also found in the UV/vis spectra of the three compounds (Fig. 7).

Conclusion

Three chromophores (**1-3**) featuring benzo(*b*)indole as donating moiety and dicyanomethylene, cyanoethyl methylene and dimethyl malonate as acceptors with π-conjugate spacer have been synthesized by knoevenagel reactions. The prepared push-pull compounds have been further investigated by UV/vis absorption spectroscopy, cyclic voltammetry as well as quantum-chemical calculations. From the performed analysis, we can deduce that the optical properties of the polar push-pull molecules can be easily tuned by the appended acceptor. The absorption spectra of dyes **1-3** exhibit an intramolecular charge transfer band; which showed a positive solavotochromism in different solvents. The

emission spectra of the dyes also reveal the intramolecular charge transfer band character. These findings confirm that there is a significant electron transfer between the donating moiety and the accepting fragment through the π-conjugated core. The features of the accepting moieties, confirm their behavior as a versatile and an efficient acceptor units.

Acknowledgments. Authors are thankful to the Center of Excellence for Advanced Materials Research and the Chemistry Department at King Abdulaziz University for providing the research facilities.

References

1. Qiu, F.; Zhou, Y.; Liu, J.; Zhang, X. *Dyes & Pigments* **2006**, *71*, 37.
2. Zhang, Y.; Wang, L.; Wada T.; Sasabe, H. *Macromolecules* **1996**, *29*, 1569.
3. Gatica, N.; Marcelo, G.; Mendicuti, F. *Polymer* **2006**, *47*, 7397.
4. Mori, T.; Kijima, M. *Eur. Poly. J.* **2009**, *45*, 1149.
5. Kim, K.; Jeong, S.; Kim, C.; Ham, J.; Kwon, Y.; Choi, B.; Han, Y. S. *Synthetic. Metals* **1999**, *159*, 1870.
6. Uekawa, M.; Miyamoto, Y.; Ikeda, H.; Kaifu, K.; Ichi, T.; Nakaya, T. *Thin Solid Film* **1999**, *352*, 185.
7. Li, S.; Wu, J.; Tian, Y.; Tang, T.; Jiang, M.; Fun, H. K.; Chantrapromma, S. *Optical. Materials* **2006**, *28*, 897.
8. Choi, M.; Kim, Y.; Ha, C. *Progress in Polymer Science* **2008**, *33*, 581.
9. Biswas, M.; Das, S. K. *European Polymer J.* **1982**, *18*, 945.
10. Liu, Z.; Cao, D.; Chen, Y.; Fang, O. *Dyes & Pigments* **2010**, *86*, 63.
11. Li, J.; Peng, M.; Zhang, L.; Wu, L.; Wang, B.; Tung, C. *J. Photochem. Photobiol A: Chem.* **2002**, *150*, 101.
12. Asiri, A. M. *Dyes &Pigments* **1999**, *42*, 209.
13. Cho, M. J.; Kim, J. Y.; Kim, J. H.; Lee, S. H.; Dalton, L. R.; Choi, D. H. *Bull. Korean Chem. Soc*. **2005**, *26*, 77.
14. Zhang, H.; Wan, X.; Xue, X.; Li, Y.; Chen, Y. *Eur. J. Org. Chem.* **2010**, 1681.
15. Thomas, K. R. J.; Lin, J. T.; Velusamy, M.; Tao, Y. T.; Chues, C. H. *Adv. Fundt. Mater.* **2004**, *14*, 83.
16. Raimundo, J. M.; Blanchard, P.; Brisset, H.; Akoudad, S.; Roncali, J. *Chem. Commun.* **2000**, 939.
17. El-Hallag, I. S.; El-Daly, S. A. *Bull. Korean Chem. Soc.* **2010**, *31*, 989.
18. El-Hallag, I. S.; Ghoneim, M. M.; Hammam, E. *Anal. Chim. Acta* **2000**, *414*, 173.
19. El-Hallag, I. S. *Rev. Chim. (Bucharest)* **2011**, *62*, 27.
20. Turro, N. J. *Modern Molecular Photochemistry*; University Science Books: 1991; p 88.
21. Kumar, G. A.; Unnikrishon, N. V. *Solid State Commun*. **1994**, *29*, 1049.
22. Kumar, G. A.; Unnikrishan, N. V. *J. Photochemistry & Photobiologe A: Chemistry* **2001**, *144*, 104.
23. Briks, J. B. *Photophysics of Aromatic Molecules Wiles*; London 1970; p 88
24. Song, H. C.; Chen, Y. W.; Zheng, X. L.; Ying, B. N. *Spectrochim. Acta Part A* **2001**, *57*, 1717.